Research Article

Journal of Environmental Nanotechnology

# Green-synthesized $Al_2O_3$ Nanoparticle-enhanced Rubber Seed–Avocado Seed Hybrid Biodiesel for CI Engine Performance: Experimental Investigation and CatBoost-based Machine Learning Prediction

K. Gopalakrishnan[1*], N. Vinodh[2], S. Arunkumar[3], P. Saveetha[4], K. Uma[5] and R. Girimurugan[3]
[1]Department of Computer Science and Business Systems, Dr. N.G.P. Institute of Technology, Coimbatore, TN, India
[2]Department of Management Studies, Prathyusha Engineering College, Tiruvallur, TN, India
[3]Department of Mechanical Engineering, Nandha College of Technology, Perundurai, TN, India
[4]Department of Information Technology, Erode Sengunthar Engineering College, Erode, TN, India
[5]Department of Mechanical Engineering, Government College of Engineering, Erode, TN, India
Received: 31.07.2026 Accepted: 29.08.2026 Published: xx.xx.xxxx
*gopalakrishnanbtech1@gmail.com,

## ABSTRACT

The relatively high viscosity and lower heating value of biodiesel can reduce brake thermal efficiency and increase fuel consumption in compression ignition (CI) engines. The novelty of this study lies in integrating rubber seed–avocado seed hybrid biodiesel, green-synthesized $Al_2O_3$ nanoparticles, and CatBoost-based prediction within a single experimental framework. Hybrid biodiesel was prepared from equal proportions of rubber seed and avocado seed oils, while $Al_2O_3$ nanoparticles were synthesized using *Syzygium cumini* leaf extract and aluminium nitrate nonahydrate as the precursor. Nanoparticle formation was preliminarily supported by a UV–visible absorption band near 350 nm and an Al–O vibration near 595 cm$^{-1}$ in the FTIR spectrum, while DLS indicated an average particle size of 30 ± 5 nm. The reported engine-performance analysis focused on B25 and B50 blends, with and without 40 ppm $Al_2O_3$ nanoparticles, using a single-cylinder CI engine operated at 1500 rpm, compression ratios of 15:1, 17:1, and 19:1, and loads of 2, 5, 8, and 11 kg. Engine performance was evaluated using brake thermal efficiency (BTE) and brake-specific fuel consumption (BSFC). At 11 kg load, B25 + $Al_2O_3$ increased BTE by 6.10% and reduced BSFC by 6.13% at 19:1. B50 + $Al_2O_3$ produced a maximum BTE improvement of 6.05% at 17:1 and a maximum BSFC reduction of 7.12% at 19:1. Separate CatBoost models were developed using biodiesel percentage, $Al_2O_3$ concentration, compression ratio, engine load, lower heating value, and brake power. The models achieved $R^2$ values of 0.9967 for BTE and 0.9918 for BSFC. Within the investigated operating conditions, 40 ppm $Al_2O_3$ improved the measured performance of B25 and B50, while CatBoost accurately predicted their BTE and BSFC. Therefore, the developed nano-biodiesel and CatBoost framework has potential application in predicting and improving the performance of biodiesel-fuelled CI engines under comparable operating conditions.

**Keywords:** Green synthesis; Machine learning; Sustainability; Biodiesel; Brake thermal efficiency

Article in Press

## 1. INTRODUCTION

The increasing depletion of petroleum resources, rapid growth in stringent environmental regulations, and global energy demand have intensified search for renewable and sustainable alternative fuels for CI engines. Biodiesel has emerged as one of the most promising substitutes because of its renewable origin, biodegradability, oxygenated molecular structure, and compatibility with conventional diesel engines. Nevertheless, the relatively high viscosity, inferior combustion, and lower heating value characteristics of biodiesel compared with petroleum diesel often result in reduced engine efficiency and increased fuel consumption. Consequently, recent research has focused on developing hybrid biodiesel feedstocks, nanoparticle-assisted fuel additives, advanced combustion strategies, and intelligent prediction techniques to overcome these limitations and improve engine performance. Accordingly, the present study focuses on three complementary strategies: combining two non-edible biodiesel feedstocks to develop a hybrid fuel, incorporating $Al_2O_3$ nanoparticles to enhance fuel performance, and applying machine learning to predict engine responses under varying operating conditions.

Among the numerous non-edible feedstocks investigated for biodiesel production, rubber seed oil and avocado seed oil have attracted increasing attention because of their favorable fatty acid composition, widespread availability, and ability to produce biodiesel with desirable physicochemical properties. Avocado seed oil biodiesel synthesized using a CaO catalyst derived from blood cockle shells achieved an optimum biodiesel of 96% with 99.83% methyl ester, a density of 865 kg $m^{-3}$, acid value of 0.56 mg KOH $g^{-1}$, kinematic viscosity of 2.5 cSt, and a heating value of 9871.6 kcal $kg^{-1}$, demonstrating its suitability as a high-quality renewable fuel (Suprihatin *et al.* 2024). Similarly, carbon-supported CuO nanoparticles effectively catalyzed the esterification and transesterification of avocado seed oil by reducing the free fatty acid content from 8.2–10.2% to below 1%, confirming the high catalytic efficiency and favorable reaction kinetics of nanostructured catalysts for biodiesel production (Sasikumar *et al.* 2022). Previous investigations confirm that avocado and rubber seed oils are viable biodiesel feedstocks; however, considerably less attention has been given to their combined use as a 1:1 hybrid biodiesel feedstock, particularly with nanoparticle-assisted CI-engine performance evaluation. Furthermore, a CuO–$Al_2O_3$ nanocomposite catalyst optimized through Response Surface Methodology produced 96.9% biodiesel yield from Carica papaya seed oil under optimized operating conditions while maintaining over 95% catalytic activity after five reuse cycles, demonstrating excellent catalytic efficiency and long-term reusability (Dheenathayalan *et al.* 2025).

To reduce dependence on conventional nanoparticle-processing chemicals, the present study employs *Syzygium cumini* leaf extract during $Al_2O_3$ nanoparticle synthesis. Plant-derived phenolic and other oxygen-containing phytochemical constituents can participate in precursor complexation, nucleation, and surface stabilization during particle formation. Thus, the plant-assisted route introduces a sustainability-oriented component into the preparation of the $Al_2O_3$ additive used at 40 ppm in the hybrid biodiesel. Incorporation of metal oxide NPs into biodiesel had become an effective strategy for improving combustion efficiency because nanoparticles possess high thermal conductivity, catalytic activity, and oxygen buffering characteristics that promote rapid fuel oxidation and enhanced heat transfer. Among metal-oxide additives, $Al_2O_3$ is attractive because of its high thermal conductivity, large active surface area, and catalytic characteristics. When adequately dispersed in biodiesel, $Al_2O_3$ nanoparticles can enhance heat transfer and promote oxidation reactions, potentially improving fuel conversion and reducing incomplete-combustion losses. Nevertheless, these effects depend on nanoparticle concentration and dispersion; therefore, the present investigation employs a controlled 40 ppm $Al_2O_3$ loading and evaluates its influence primarily through measured BTE and BSFC. The addition of 75 ppm $Al_2O_3$ nanoparticles to *Styrax officinalis* biodiesel increased BTE from 31.2% to 34.1%; qualitative emission wording was omitted where exact numerical changes were unavailable (Oni *et al.* 2022). Likewise, $Al_2O_3$/CuO hybrid nanoparticles incorporated into tobacco seed biodiesel and optimized through Response Surface Methodology achieved a biodiesel yield of 95.58%, while the optimized B15AC100 blend reduced CO by 73.57%, HC by 76.10%, $CO_2$ by 11.63%, and $NO_x$ by 7.49%, demonstrating remarkable emission improvements without compromising engine performance (Siam *et al.* 2026). Furthermore, rubber seed oil biodiesel blended with hydrogen and $Al_2O_3$ nanoparticles exhibited superior combustion stability while reducing CO (12.12%), HC (12.12%), $CO_2$ (8.13%), $NO_x$ (20.46%), and smoke emissions (14.11%), highlighting the synergistic benefits of combining hydrogen enrichment with nanoparticle-assisted combustion (Thangam *et al.* 2026).

Recent biodiesel-engine research increasingly combines fuel modification with data-driven prediction to improve performance assessment. Nanoparticle-assisted biodiesel studies have demonstrated improvements in BTE and BSFC, while ML models such as ANN, SVR, XGBoost, and CatBoost provide efficient tools for modelling nonlinear relationships between fuel composition, engine operating conditions, and performance responses (Bukkarapu and Krishnasamy, 2026). These findings support the integration of nanoparticle-enhanced biodiesel experiments with machine-learning prediction in the present investigation (Kannappan *et al.* 2023). Similarly, hydrogen-assisted dual-fuel operation of Mahua biodiesel with $Al_2O_3$–$TiO_2$ and $CeO_2$–MWCNT hybrid nanoparticles enhanced BTE by 8–14%, reduced BSFC by 10–18%, and decreased CO by 32%, HC by 35%, and smoke emissions by 45%, while XGBoost achieved prediction accuracies exceeding $R^2 = 0.99$, enabling effective multi-objective optimization of emissions and engine performance (Bilal *et al.* 2026). In addition, naturally derived antioxidants obtained from eucalyptus, Pongamia leaf and neem extracts improved the oxidation stability and combustion behavior of Mango seed biodiesel with the optimized fuel blend reducing HC by 22.22%, CO by 36.84%, smoke opacity by 13.83%, and $NO_x$ by 17.72%, while shortening ignition delay by 44.95% and increasing peak cylinder pressure to 74 bar (Dhairiyasamy *et al.* 2025).

Besides fuel modification, advanced combustion concepts and optimization techniques have been extensively explored to improve combustion efficiency while minimizing exhaust emissions. Reactivity Controlled Compression Ignition (RCCI) using Jatropha curcas biodiesel and gasoline improved brake thermal efficiency by 0.2–1.2%, increased the net heat release rate by 11.3–44.6%, and reduced $NO_x$ emissions by 24.40–43.74% together with soot emissions by 31.28–52.57%, while VIKOR optimization identified optimum operating conditions for simultaneous performance and emission improvement (Sengodan *et al.* 2025). Likewise, rapeseed biodiesel and Pongamia pinnata blended with n-butanol and optimized using Response Surface Methodology reduced $NO_x$ emissions by 7.07% and 6.58%, respectively, whereas Artificial Neural Network models achieved superior prediction accuracies ranging from 87.92% to 98.83% compared with conventional regression approaches (Al Zubi *et al.*

Article in Press

2024). CatBoost was selected because gradient-boosted decision trees can model nonlinear interactions among fuel blend, engine load, and compression ratio without requiring a predefined functional relationship. Its ordered boosting and regularization mechanisms also help control overfitting in comparatively limited structured datasets. Accordingly, CatBoost was employed to predict the two principal performance responses, BTE and BSFC (Li *et al.* 2025). The rapid advancement of ML and ANN has provided efficient alternatives to conventional statistical methods for predicting biodiesel production and engine performance. ML models, including SVR, ANN, and ANFIS, have been successfully employed to predict diesel engine torque and $NO_x$ emissions, with SVR demonstrating the highest prediction accuracy and robustness for biodiesel engine applications (Rajakannu *et al.* 2025).

Existing studies have mainly investigated single-feedstock biodiesels, nanoparticle fuel additives, or machine-learning prediction independently. However, the combined use of equal proportions of rubber seed and avocado seed biodiesel, 40 ppm green-synthesized $Al_2O_3$ nanoparticles, and CatBoost-based prediction of BTE and BSFC has not been systematically reported. The present study addresses this gap by integrating hybrid-feedstock utilization, green nanoparticle-assisted fuel modification, experimental CI-engine evaluation, and machine-learning prediction within a unified framework. Accordingly, this study aims to: (i) determine the physicochemical characteristics of rubber seed oil, avocado seed oil, and the resulting hybrid biodiesel; (ii) synthesize and characterize green $Al_2O_3$ nanoparticles using *Syzygium cumini* leaf extract; (iii) investigate the influence of 40 ppm $Al_2O_3$ nanoparticle-enriched biodiesel blends on BTE and BSFC of a CI engine under different loads and compression ratios of 15:1, 17:1, and 19:1; and (iv) develop CatBoost models for predicting BTE and BSFC and assessing engine-performance trends.

## 2. MATERIALS AND METHODOLOGY

### 2.1 Preparation of Hybrid Biodiesel

Rubber seed oil and avocado seed oil were blended in an equal 1:1 proportion, and a two-stage esterification–transesterification procedure was followed with modifications (Yatish *et al.* 2021). Because rubber seed oil contained 4.36% free fatty acids, the blended oil was initially subjected to acid-catalysed esterification. Methanol was added at a methanol-to-oil molar ratio of 6:1, followed by 5 mL of $H_2SO_4$ per batch. The mixture was maintained at 60 °C and stirred at 600 rpm for 60 min. After completion of acid esterification, the mixture was allowed to settle, and the methanol–water phase was separated. The acid-treated oil was subsequently subjected to alkaline transesterification using 7 g of NaOH dissolved in 150 mL of methanol. $H_2SO_4$ was used during the initial esterification stage to reduce the free fatty acid content and minimize soap formation, whereas NaOH was employed during the subsequent transesterification stage to convert triglycerides into fatty acid methyl esters. Thus, the acid and alkaline catalysts were used sequentially rather than simultaneously. The reaction was maintained at 60 °C and 600 rpm for 2 h. The resulting mixture was transferred to a separating funnel and allowed to settle for 1 h to separate the glycerol and biodiesel phases. The recovered biodiesel was repeatedly washed with distilled water until the wash water became clear and reached neutral pH. Finally, the purified biodiesel was dried in a hot-air oven at 105 °C until constant mass was obtained. The resulting hybrid biodiesel was then used for the preparation of $Al_2O_3$ nanoparticle-enhanced fuel blends, where the nanoparticles were synthesized using *Syzygium cumini* leaf extract and aluminium nitrate nonahydrate ($Al(NO_3)_3 \cdot 9H_2O$) as the aluminium precursor.

The biodiesel yield was calculated using Eq. (1):

$$\text{Biodiesel yield (\%)} = \frac{\text{mass of dried biodiesel (g)}}{\text{initial mass of blended oils (g)}} \times 100 \; ... \; (1)$$

The biodiesel yield was determined gravimetrically as the mass of purified and dried biodiesel relative to the initial mass of blended feedstock oils.

### 2.2 Physicochemical Characteristics of Feedstock Oils and Hybrid Biodiesel

Fuel properties were evaluated using the corresponding standard procedures: density by ASTM D4052, kinematic viscosity by ASTM D445, flash point by ASTM D93, cetane number by ASTM D613, calorific value by ASTM D240, moisture content by ASTM D6304, acid value by ASTM D664, and pour point by ASTM D97. For the feedstock oils, free fatty acid content was determined by ASTM D5555, saponification value by ISO 3657, and iodine value by ISO 3961. The resulting biodiesel properties were compared with the specification limits of ASTM D6751 and EN 14214 (Sai *et al.* 2022).

Table 1 summarizes the fatty acid composition of the selected feedstock oils. Major fatty acids, including linoleic, oleic, stearic, and palmitic acids, significantly influence oxidation stability, combustion characteristics, cold-flow behavior, and overall fuel quality. The balanced fatty acid profile of avocado seed oil and rubber seed oil makes them promising renewable feedstocks for producing hybrid biodiesel with desirable fuel properties. The principal physicochemical characteristics of feedstock oils were presented in Table 2. Parameters like free acid value, fatty acid content, viscosity, saponification value, flash point, density, and moisture provide important information regarding transesterification efficiency, storage stability, and biodiesel production potential. These properties were

Article in Press

considered when selecting the operating conditions for biodiesel synthesis.

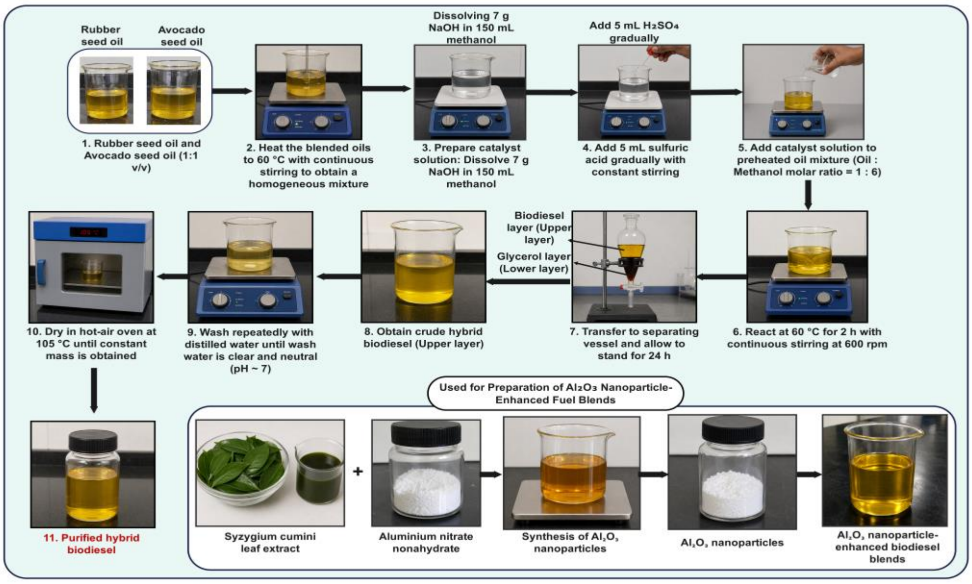


**Fig. 1: Schematic representation of hybrid biodiesel production from rubber seed and avocado seed oils and the preparation of $Al_2O_3$ nanoparticle-enhanced biodiesel blends**

**Table 1. Fatty acid composition and significance of rubber seed oil and avocado seed oil**

| Fatty Acid | Avocado Seed Oil (%) | Rubber Seed Oil (%) | Significance |
|---|---|---|---|
| Palmitic acid (C16:0) | 19.32 | 10.84 | Improves cetane number and oxidation stability |
| Stearic acid (C18:0) | 0.68 | 8.91 | Enhances storage stability |
| Oleic acid (C18:1) | 57.84 | 24.76 | Improves oxidative stability and combustion |
| Linoleic acid (C18:2) | 15.46 | 37.58 | Enhances cold-flow characteristics |
| Linolenic acid (C18:3) | 1.18 | 16.12 | Influences oxidation resistance |
| Others | 5.52 | 1.79 | Minor fatty acid constituents |

**Table 2. Physicochemical properties of rubber seed oil and avocado seed oil**

| Property | Avocado Seed Oil | Rubber Seed Oil | Significance |
|---|---|---|---|
| Density at 15 °C (kg m⁻³) | 905 | 912 | Fuel energy content |
| Acid value (mg KOH g⁻¹) | 2.86 | 8.72 | Indicates free fatty acid level |
| Kinematic viscosity at 40 °C (mm² s⁻¹) | 35.61 | 39.82 | Atomization characteristics |
| Saponification value (mg KOH g⁻¹) | 192.8 | 189.4 | Biodiesel conversion potential |
| Free fatty acid content (% as oleic acid) | 1.43 | 4.36 | Determines pretreatment requirement |
| Iodine value (g $I_2$ 100 g⁻¹) | 86.5 | 132.6 | Degree of unsaturation |
| Flash point (°C) | 272 | 248 | Storage safety |
| Moisture content (wt.%) | 0.08 | 0.11 | Influences transesterification efficiency |

A comparison of fuel characteristics of diesel fuel and the prepared hybrid biodiesel is presented in Table 3. Important fuel quality parameters, including density, kinematic viscosity, cetane number, flash point, pour point, and calorific value, were evaluated to determine the suitability of the produced hybrid biodiesel for compression ignition engine operation (Kannappan *et al.* 2025). The measured values satisfied the recommended biodiesel standards, confirming the effectiveness of the transesterification process.

Article In Press

**Table 3. Properties of hybrid biodiesel and diesel**

| Property | Hybrid Biodiesel | ASTM D6751 | Diesel |
|---|---|---|---|
| Density at 15 °C (kg $m^{-3}$) | 876 | 860–900 | 835 |
| Kinematic viscosity at 40 °C ($mm^2\ s^{-1}$) | 4.52 | 1.9–6.0 | 2.84 |
| Flash point (°C) | 168 | >130 | 68 |
| Cetane number (dimensionless) | 54 | ≥47 | 48 |
| Calorific value (MJ $kg^{-1}$) | 40.18 | — | 43.52 |
| Moisture content (wt.%) | 0.021 | ≤0.05 | — |
| Acid value (mg KOH $g^{-1}$) | 0.31 | ≤0.50 | — |
| Pour point (°C) | −6 | — | −18 |

Physicochemical properties of diesel, hybrid biodiesel blends, and $Al_2O_3$ NPs-enhanced biodiesel blends are presented in Table 4. Hybrid biodiesel blends (B25, B50, B75, and B100) were prepared both without nanoparticles and with 40 ppm $Al_2O_3$ nanoparticles synthesized using *Syzygium cumini* leaf extract and aluminium nitrate nonahydrate ($Al(NO_3)_3 \cdot 9H_2O$) as the aluminium precursor. Measured properties included calorific value, density, relative viscosity, flash point and kinematic viscosity.

**Table 4. Physicochemical properties of diesel and hybrid biodiesel blends without $Al_2O_3$ nanoparticles**

| Blend | Kinematic Viscosity at 40 °C ($mm^2\ s^{-1}$) | Density at 15 °C (g $cm^{-3}$) | Calorific Value (kJ $kg^{-1}$)e | Relative Viscosity | Flash Point (°C) |
|---|---|---|---|---|---|
| D100 | 2.84 | 0.834 | 43520 | 4.12 | 68 |
| B25 | 3.21 | 0.842 | 42680 | 4.56 | 76 |
| B50 | 3.66 | 0.851 | 41840 | 5.03 | 95 |
| B75 | 4.08 | 0.862 | 41020 | 5.48 | 132 |
| B100 | 4.52 | 0.876 | 40180 | 5.96 | 168 |

**Table 5. Physicochemical properties of hybrid biodiesel blends containing 40 ppm $Al_2O_3$ nanoparticles**

| Blend | Kinematic Viscosity at 40 °C ($mm^2\ s^{-1}$) | Density at 15 °C (g $cm^{-3}$) | Calorific Value (kJ $kg^{-1}$)e | Relative Viscosity | Flash Point (°C) |
|---|---|---|---|---|---|
| B25 + $Al_2O_3$ | 3.12 | 0.843 | 42680 | 4.48 | 76 |
| B50 + $Al_2O_3$ | 3.56 | 0.852 | 41840 | 4.95 | 95 |
| B75 + $Al_2O_3$ | 3.96 | 0.863 | 41020 | 5.34 | 132 |
| B100 + $Al_2O_3$ | 4.39 | 0.877 | 40180 | 5.82 | 168 |

The addition of 40 ppm $Al_2O_3$ produced a modest reduction in kinematic viscosity: from 3.21 to 3.12 $mm^2\ s^{-1}$ for B25, 3.66 to 3.56 $mm^2\ s^{-1}$ for B50, 4.08 to 3.96 $mm^2\ s^{-1}$ for B75, and 4.52 to 4.39 $mm^2\ s^{-1}$ for B100. These changes correspond to reductions of approximately 2.80%, 2.73%, 2.94%, and 2.88%, respectively. In contrast, density changed by only 0.001 g $cm^{-3}$, and the measured calorific values remained unchanged. Therefore, the results demonstrate a viscosity-related modification rather than a general improvement in all fuel properties. Furthermore, incorporation of $Al_2O_3$ nanoparticles produced measurable improvements in the fuel properties of the hybrid biodiesel blends. Slight reductions in kinematic viscosity together with stable density and calorific value are expected to promote improved fuel atomization, more efficient combustion, and enhanced engine performance. The observed improvements suggest that nanoparticle addition contributes positively to fuel quality without adversely affecting the fundamental physicochemical characteristics required for diesel engine applications.

The fuel property evaluation presented in Tables 1–5 confirms that hybrid biodiesel from rubber seed oil and avocado seed oil, together with $Al_2O_3$ nanoparticles synthesized using *Syzygium cumini* leaf extract, exhibits physicochemical properties suitable for compression ignition engines (Borsato *et al.* 2026). The combination of acceptable density, moderate viscosity, high flash point, and adequate calorific value provides favorable conditions for efficient combustion and supports application of nanoparticle-assisted hybrid biodiesel as sustainable alternative fuel.

## 2.3 Green Synthesis of Aluminum Oxide Nanoparticles

Aluminum oxide nanoparticles were synthesized using physical, biological, and chemical approaches. Chemical techniques generally involve precipitation, sol-gel, and hydrothermal techniques, whereas physical approaches include laser ablation and thermal evaporation. Among these routes, green synthesis has attracted considerable attention because it utilizes naturally occurring phytochemicals as reducing, complexing, and stabilizing agents, thereby minimizing hazardous chemicals and improving environmental sustainability (Amale *et al.* 2026).

Fresh *Syzygium cumini* leaves were washed with tap water followed by distilled water to eliminate dust and surface contaminants (Munir *et al.* 2024). Approximately 10 g of clean leaves were shade-dried for 3 days, pulverized into a fine powder, and sieved to obtain a uniform particle size for efficient extraction. The powdered leaves were mixed with 100 mL of DIW in a 200 mL flask and heated at 60 °C for 60 min with continuous stirring. After cooling to ambient

Article in Press

temperature, the extract was filtered through filter paper and stored for subsequent nanoparticle synthesis.

An aqueous precursor solution was prepared by dissolving ($Al(NO_3)_3 \cdot 9H_2O$) in double-distilled water to obtain 0.1 M solution. Subsequently, 10 mL of the *Syzygium cumini* leaf extract was slowly introduced into 90 mL of the precursor solution while stirring continuously at temperature below 50 °C for 90 min. During reaction, the phytochemical constituents present in the extract promoted the hydrolysis of aluminium ions and facilitated the nucleation and growth of $Al_2O_3$ nanoparticles. Polyphenols, flavonoids, and other oxygen-containing constituents of *Syzygium cumini* contain hydroxyl and carbonyl groups capable of coordinating $Al^{3+}$ ions. These groups can facilitate precursor hydrolysis and nucleation while adsorbed organic molecules restrict particle growth and agglomeration. During calcination at 500 °C for 2 h, the organic residues are decomposed and the aluminium hydroxide intermediate is converted into aluminium oxide. The shifts in the O–H band from 3390 to 3445 $cm^{-1}$ and the carbonyl-associated band from 1640 to 1635 $cm^{-1}$ provide preliminary evidence of phytochemical interaction; however, they do not independently establish the $Al_2O_3$ crystalline phase. Formation of the nanoparticles was indicated by the gradual appearance of a milky white suspension.

The reaction mixture was ultrasonicated for 1 hour to improve particle dispersion and minimize agglomeration (Saravanakumar *et al.* 2025). The synthesized nanoparticles were collected by centrifugation at 14,000 rpm for 10 min, washing with ethanol and distilled water to remove residual impurities. The purified precipitate was dried in a hot-air oven and finally calcined at 500 °C for 2 h to obtain crystalline $Al_2O_3$ nanoparticles.

A hybrid biodiesel was prepared by blending rubber seed oil biodiesel and avocado seed oil biodiesel at an equal 1:1 proportion. To prepare the nano-fuel, 40 ppm $Al_2O_3$ NPs were first dispersed in a small quantity of the hybrid biodiesel together with a suitable surfactant to improve dispersion stability. The suspension was subsequently mixed with the remaining biodiesel and ultrasonicated at 40 kHz and 200 W for 50 min at ambient temperature to achieve uniform nanoparticle distribution. DLS analysis showed an average particle size of 30 ± 5 nm. The prepared nano-biodiesel exhibited excellent dispersion stability without noticeable sedimentation or phase separation during 48 h of storage, indicating good colloidal stability for engine performance evaluation.

## 2.4 FTIR and UV–Visible Spectroscopic Analysis

Formation of $Al_2O_3$ nanoparticles synthesized using *Syzygium cumini* leaf extract was initially examined by UV spectroscopy over a wavelength range of 200–800 nm using a Shimadzu UV-1900i UV–Visible Spectrophotometer with a resolution of 1 nm.

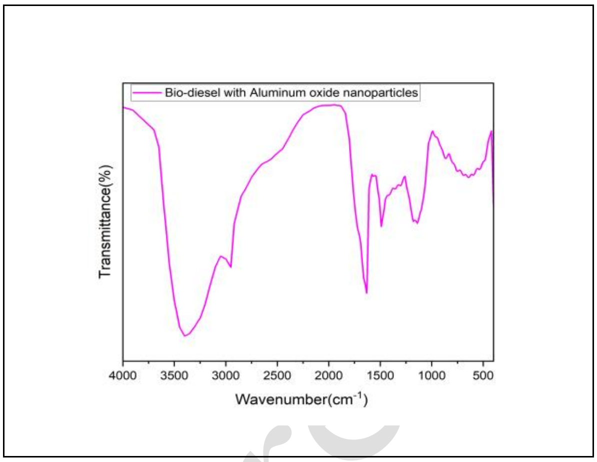


**Fig. 2: FTIR spectrum of $Al_2O_3$ nanoparticle-enhanced hybrid biodiesel**

FTIR was employed to identify functional groups responsible for reduction, stabilization, and capping of $Al_2O_3$ nanoparticles synthesized from *Syzygium cumini* leaf extract. Spectra were recorded between 4000 and 400 $cm^{-1}$ using a Bruker ALPHA II FTIR spectrometer equipped with an ATR diamond crystal and a spectral resolution of 4 $cm^{-1}$.

For nano-fuel preparation, 40 ppm $Al_2O_3$ nanoparticles together with a suitable nonionic surfactant were dispersed into 500 mL of hybrid biodiesel prepared from rubber seed oil and avocado seed oil. The suspension was ultrasonicated at 40 kHz and 200 W for 50 min at ambient temperature to obtain a homogeneous dispersion before FTIR characterization.

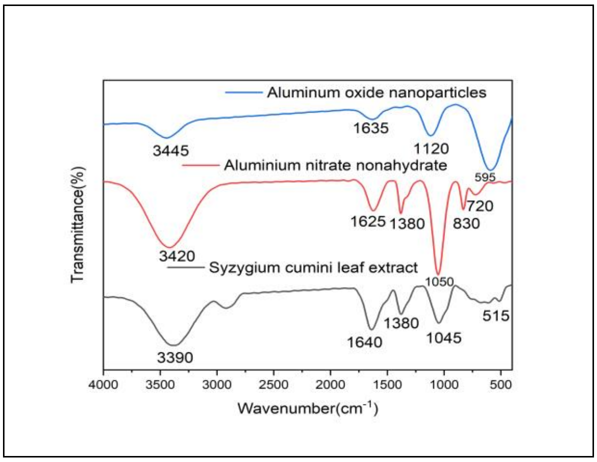


**Fig. 3: FTIR spectra of *Syzygium cumini* leaf extract, aluminium nitrate nonahydrate precursor and synthesized $Al_2O_3$ nanoparticles**

The FTIR spectrum of the nano-biodiesel (Figure 2) exhibited a broad absorption band at 3420

Article In Press

$cm^{-1}$, corresponding to O–H stretching linked with hydroxyl groups of residual phytochemicals and absorbed moisture. Strong bands observed at 2960 and 2925 $cm^{-1}$ were assigned to symmetric and asymmetric C–H stretching of aliphatic hydrocarbons. A distinct absorption peak at 1740 cm ¹ confirmed the ester carbonyl (C=O) stretching vibration characteristic of biodiesel methyl esters. Peaks located at 1605 $cm^{-1}$ represented C=C stretching vibrations, whereas absorption bands at 1450 and 1375 $cm^{-1}$ were attributed to $CH_2$ and $CH_3$ modes. Strong bands appearing at 1240, 1160, and 1050 $cm^{-1}$ corresponded to C–O stretching of ester functional groups. Characteristic Al–O lattice vibration was identified near 620 $cm^{-1}$, confirming successful addition of $Al_2O_3$ nanoparticles within biodiesel matrix.

FTIR spectra of the *Syzygium cumini* leaf extract, aluminium nitrate nonahydrate [$Al(NO_3)_3 \cdot 9H_2O$], and prepared $Al_2O_3$ nanoparticles are shown in Fig. 3. The leaf extract showed a wide band of O–H stretching at 3390 $cm^{-1}$, suggesting the presence of hydroxyl-containing phytochemicals. It has bands in the region of 1380, 1640, and 1045 cm-1, which were assigned to vibrations of carbonyl groups, aromatic groups, and C–O, respectively. The presence of a low-wavenumber band was noticed near 515 $cm^{-1}$. Aluminium nitrate nonahydrate exhibited bands at 3420, 1625, 1380, 1050, 830, and 720 $cm^{-1}$. The strong band at 1380 $cm^{-1}$ was mostly attributed to vibrations of the nitrate ion. After the formation of the nanoparticles, the $Al_2O_3$ spectrum exhibited bands at 3445, 1635, 1120, and 595 $cm^{-1}$. The unique band at 595 $cm^{-1}$ was attributed to Al–O lattice vibrations, which is consistent with the formation of $Al_2O_3$ nanoparticles. The changes in O–H stretching (3390–3445 $cm^{-1}$) and carbonyl-associated bands (1640–1635 $cm^{-1}$), along with the changes in the band intensities, indicate that plant phytochemicals are involved in complexation of aluminium ions and stabilization of nanoparticles. UV–vis spectra in Fig. 4 and 5 were obtained to analyze the inclusion of key absorption peaks and absorbing species.

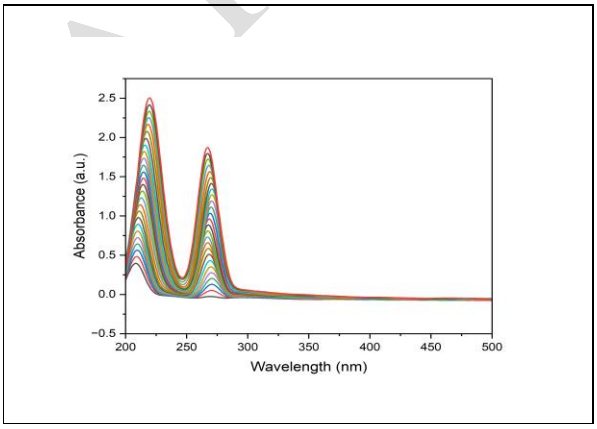


**Fig. 4: UV–visible absorption spectrum of *Syzygium cumini* leaf extract and synthesized $Al_2O_3$ nanoparticles**

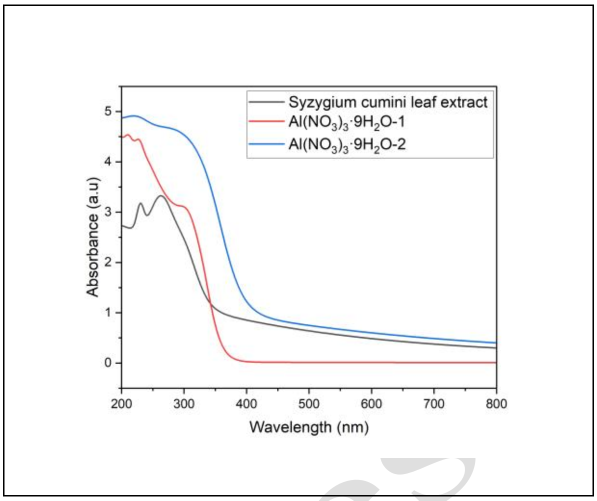


**Fig. 5: UV–visible absorption spectra of aluminium nitrate nonahydrate solution before and after $Al_2O_3$ nanoparticle synthesis**

The optical properties of the synthesized $Al_2O_3$ nanoparticles were further investigated by UV–visible spectroscopy within the wavelength range of 200–800 nm. Unlike noble metal nanoparticles, $Al_2O_3$ nanoparticles do not exhibit surface plasmon resonance. Instead, the absorption spectrum showed a strong band in the ultraviolet region arising from electronic transitions associated with aluminium oxide.

As illustrated in Figures 4 and 5, the *Syzygium cumini* leaf extract exhibited an intense absorption peak near 270 nm, originating from phenolic and flavonoid compounds. The precursor solution containing aluminium nitrate nonahydrate ($Al(NO_3)_3 \cdot 9H_2O$) displayed only weak absorption throughout the visible region. After synthesis, a pronounced absorption maximum appeared at approximately 350 nm, indicating a change in the optical characteristics of the precursor system that is consistent with nanoparticle formation. However, this band alone does not definitively confirm the $Al_2O_3$ crystalline phase. The absence of absorption bands above 400 nm indicates that no metallic nanoparticles were produced during the synthesis process. The observed spectral variation between the precursor solution and the nanoparticle suspension reflects the conversion of aluminium ions into stable oxide nanoparticles. Visual observation also supported nanoparticle formation through the gradual transformation of the reaction mixture into a milky white suspension, consistent with the successful synthesis of $Al_2O_3$ NPs.

## 2.5 Engine Experimental Setup

Performance properties of the prepared hybrid biodiesel fuels were evaluated using a single-cylinder, four-stroke, direct-injection variable compression ratio diesel engine (Apex Innovations, Model: 661, India)

Article In Press

coupled with an eddy-current dynamometer(Renish and Amala, 2024). The engine was operated at a constant speed of 1500 rpm, while brake loads of 2, 5, 8, and 11 kg were applied to investigate the influence of operating conditions on engine performance. Test fuels consisted of diesel (D100), hybrid biodiesel blends (B25, B50, B75, and B100), and their corresponding 40 ppm $Al_2O_3$ nanoparticle-enhanced blends. A total of nine fuel conditions were investigated: D100; B25, B50, B75, and B100 without nanoparticles; and B25, B50, B75, and B100 containing 40 ppm $Al_2O_3$. Each of the nine fuel conditions was tested at three compression ratios (15:1, 17:1, and 19:1) and four brake loads (2, 5, 8, and 11 kg) at a constant speed of 1500 rpm. Therefore, the experimental design comprised 9×3×4=108 operating conditions.

The hybrid biodiesel was prepared from equal proportions of rubber seed and avocado seed oil, whereas $Al_2O_3$ NPs were synthesized through a green route using *Syzygium cumini* leaf extract with aluminium nitrate nonahydrate ($Al(NO_3)_3 \cdot 9H_2O$) as the aluminium precursor. To ensure a valid comparison among all test fuels, identical fuel injection parameters, including duration, injection pressure, and timing, were maintained throughout the experiments. Fuel injection was fixed at 23° before top dead center for every operating condition. Fuel consumption was recorded over a 60 s interval using a glass fuel-measuring column connected to a differential-pressure transmitter with a range of 0–500 mm WC. The injector-opening pressure was maintained at 210 bar, while the injection timing was fixed at 23° before top dead centre. Before testing, the load cell was calibrated using standard weights, the fuel-flow transmitter through zero-and-span calibration, the speed sensor using a digital tachometer, and the temperature sensors using a calibrated reference thermometer. Measurement uncertainties were ±10 rpm for engine speed, ±0.1 kg for load, ±0.1 s for measurement time, and ±0.5% for fuel flow. Root-sum-square uncertainty propagation produced maximum uncertainties of approximately ±1.6% for BTE and ±1.4% for BSFC.

The experimental engine had a stroke of 110 mm, a bore of 87.5 mm, a rated output of 3.5 kW, and a displacement of 661 $cm^3$. The compression ratio was adjusted using the engine's built-in VCR mechanism and set at 15:1, 17:1, and 19:1 for the present investigation. These compression ratios were selected to evaluate combustion properties of hybrid biodiesel blends at different compression conditions while maintaining constant engine speed.

Engine loading was applied using a computer-controlled eddy-current dynamometer, allowing accurate control of brake load during testing (Dinesh *et al.* 2025). Performance parameters, including BTE and BSFC, were continuously monitored through calibrated sensors connected to a computerized data acquisition system.

Each of the 108 operating conditions was tested in 3 independent replicates. The results are reported as mean ± standard deviation, calculated using:

$$SD = \sqrt{\frac{\sum_{i=1}^{n}(x_i-\bar{x})^2}{n-1}} \quad \ldots (2)$$

where $n$ is the number of replicates. Error bars representing ±1SD have been included in the BTE and BSFC figures.

## 2.6 Machine Learning-based Prediction Using CatBoost Regression

CatBoost (Categorical Boosting) is an advanced gradient-boosting machine learning algorithm developed to improve prediction accuracy while minimizing overfitting (Modi *et al.* 2025). The algorithm constructs decision trees in a sequential manner; each new tree learns from the residual errors of previously generated trees through gradient boosting. CatBoost incorporates ordered boosting and efficient tree-growing strategies that enhance prediction accuracy, reduce prediction bias, and provide robust performance even for relatively small datasets. Owing to its high predictive capability and excellent generalization performance, CatBoost has been widely employed for nonlinear regression problems in engineering applications.

In the present study, CatBoost regression was employed to predict BTE and BSFC of a CI engine with hybrid biodiesel blends prepared from rubber seed oil methyl ester and avocado seed oil methyl ester. $Al_2O_3$ NPs synthesized through a green route using Syzygium cumini leaf extract and aluminum nitrate nonahydrate ($Al(NO_3)_3 \cdot 9H_2O$) as the aluminum precursor were dispersed into biodiesel blends at concentrations of 0 and 40 ppm.

The experimental dataset was generated from engine performance tests conducted using five fuel blends (D100, B25, B50, B75, and B100) at three ratios (15:1, 17:1, and 19:1) and four engine loads (2, 5, 8, and 11 kg), maintaining a constant engine speed of 1500 rpm. A total of 108 experimental operating conditions were used for machine learning model development.

The predictor variables included biodiesel blend percentage, $Al_2O_3$ nanoparticle concentration, compression ratio, engine load, lower heating value (LHV), and brake power, whereas BTE and BSFC were considered as target responses. Prior to model development, incomplete observations were removed, and the dataset was randomly divided into 80% training and 20% testing using a fixed random seed to ensure reproducibility. Separate CatBoost regression models were developed independently for predicting BTE and BSFC. The CatBoost hyperparameters were optimized using grid search with five-fold cross-validation. The

Article In Press

search evaluated iterations of 300, 500, and 800; tree depths of 4, 6, and 8; learning rates of 0.01, 0.05, and 0.10; and L2 regularization coefficients of 3, 5, and 7. The selected model used 500 iterations, a tree depth of 6, a learning rate of 0.05, an L2 coefficient of 3, and the RMSE loss function. A random seed of 42 was maintained for reproducibility, with early stopping after 50 rounds.

The predictive performance of the developed CatBoost models was evaluated by the coefficient of determination ($R^2$), root mean square error (RMSE), mean absolute error (MAE), and mean absolute percentage error (MAPE). Agreement between experimental and predicted values was further examined using experimental-versus-predicted scatter plots with the 45° reference line, while feature importance was performed to assess the relative influence of selected operating parameters on engine performance.

## 3. RESULTS AND DISCUSSION

### 3.1 Engine Performance Analysis

The performance of prepared hybrid biodiesel was evaluated by BTE and BSFC, which are widely recognized as primary indicators of compression ignition engine performance. Experiments were conducted using hybrid biodiesel produced from equal proportions of rubber seed and avocado seed oil, together with corresponding 40 ppm $Al_2O_3$ nanoparticle-enhanced biodiesel blends. Performance tests were carried out under different compression ratios and engine loading conditions to assess the influence of nanoparticle incorporation on combustion behavior and fuel utilization.

The performance comparison was performed at brake loads of 2, 5, 8, and 11 kg, while compression ratios of 15:1, 17:1, and 19:1 were investigated. Particular emphasis was placed on the 11 kg load because combustion efficiency, thermal conversion, and fuel consumption differences become more pronounced under high-load operating conditions, providing a reliable basis for evaluating the effectiveness of the nanoparticle-improved hybrid biodiesel. The 11 kg condition represented the maximum applied load and produced the highest brake power and thermal loading.

#### 3.1.1 Brake Thermal Efficiency

BTE represents the effectiveness with which chemical energy contained in fuel was converted into useful brake power. The $Al_2O_3$ nanoparticles in hybrid biodiesel noticeably enhanced combustion efficiency compared with the corresponding nanoparticle-free blends. The improvement was attributed to the large specific surface area and high thermal conductivity of $Al_2O_3$ nanoparticles, which promote more efficient heat transfer inside the combustion chamber and accelerate oxidation reactions during combustion.

Addition of 40 ppm $Al_2O_3$ produced modest viscosity reductions of 2.80%, 2.73%, 2.94%, and 2.88% for B25, B50, B75, and B100, respectively. These changes may modestly influence fuel flow and spray behaviour; however, improved atomization cannot be confirmed without direct spray-characterization data. Improved atomization produced a finer fuel spray and more homogeneous air-fuel mixing, leading to faster flame development, complete combustion, and higher heat release. Consequently, greater cylinder pressure and improved combustion efficiency contributed to an increase in brake thermal efficiency over the entire operating range.

The hybrid biodiesel exhibited consistent measured BTE and BSFC trends throughout the investigated operating range. These combined effects resulted in improved thermal energy conversion and demonstrated the suitability of nanoparticle-assisted hybrid biodiesel as an efficient alternative fuel for compression ignition engines.

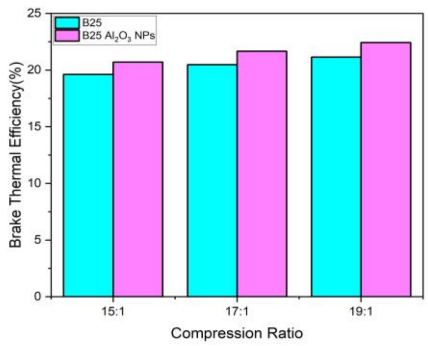


**Fig. 6: Maximum BTE of B25 and B25 + 40 ppm $Al_2O_3$ blends**

At the maximum engine load of 11 kg, the B25 + 40 ppm $Al_2O_3$ blend exhibited brake thermal efficiency values of 20.71%, 21.66%, and 22.43% at compression ratios of 15:1, 17:1, and 19:1, respectively. Under identical operating conditions, the corresponding B25 blend without nanoparticles produced BTE values of 19.62%, 20.48%, and 21.14%, respectively. The incorporation of $Al_2O_3$ nanoparticles therefore improved the maximum brake thermal efficiency by approximately 5.56%, 5.76%, and 6.10% for compression ratios of 15:1, 17:1, and 19:1, respectively. The improvement was attributed to the enhanced catalytic activity and thermal conductivity of $Al_2O_3$ NPs, which promoted finer fuel atomization, more homogeneous air-fuel mixing, and improved combustion. Furthermore, a higher compression ratio facilitated improved combustion

Article in Press

efficiency, resulting in greater heat release and effective conversion of fuel energy as useful brake power.

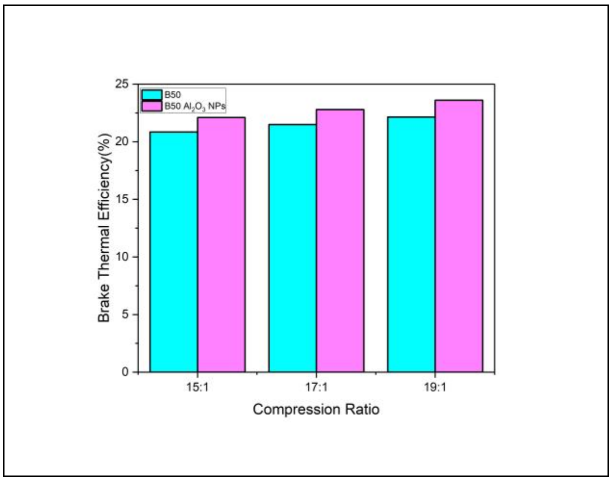


**Fig. 7: Maximum BTE comparison of B50 and B50 + 40 ppm $Al_2O_3$ blends**

Incorporation of $Al_2O_3$ nanoparticles into the hybrid biodiesel improved brake thermal efficiency by enhancing fuel atomization, promoting more homogeneous air-fuel mixing, and accelerating combustion. Large surface area and high thermal conductivity of nanoparticles facilitated improved heat transfer inside combustion chamber, resulting in higher heat release and efficient conversion of chemical energy as useful brake power. The selected nanoparticle concentration (40 ppm) provided stable combustion without causing adverse combustion phasing under high-load conditions.

Figure 7 presents comparison of maximum BTE obtained for B50 blend and B50 + 40 ppm $Al_2O_3$ blend at ratio of 15:1, 17:1, and 19:1. Maximum engine (11 kg), the B50 + 40 ppm $Al_2O_3$ blend achieved BTE values of 22.1%, 22.8%, and 22.6%, whereas the corresponding B50 blend recorded 20.85%, 21.5%, and 22.25%, respectively. The addition of $Al_2O_3$ NPs increased maximum BTE by 6.00%, 6.05%, and 1.57% for the compression ratios of 15:1, 17:1, and 19:1, respectively. The measured results demonstrate changes in BTE and BSFC only. Possible effects involving catalytic oxidation, heat transfer, spray atomization, and combustion kinetics are literature-based interpretations because spray, cylinder-pressure, ignition-delay, and heat-release measurements were not conducted. These improvements indicate that the green-synthesized $Al_2O_3$ nanoparticles, prepared using *Syzygium cumini* leaf extract and aluminium nitrate nonahydrate ($Al(NO_3)_3 \cdot 9H_2O$), enhanced combustion efficiency and thermal energy utilization, demonstrating the potential of nanoparticle-assisted hybrid biodiesel for raising CI engine performance. Similarly, hybrid $Al_2O_3/CeO_2$ nanoparticles incorporated into 20% castor biodiesel (CB20) enhanced diesel engine performance, with the CB20A50C50 blend increasing brake power by 6.14%, brake thermal efficiency by 20.38%, and reducing BSFC by up to 8.29% compared with CB20 (Tesfaye *et al.* 2023).

#### 3.1.2 Brake-specific Fuel Consumption

Incorporation of $Al_2O_3$ nanoparticles into hybrid biodiesel prepared from rubber seed oil and avocado seed oil provides an effective approach for improving fuel utilization in compression ignition engines. The enhancement mainly arises from the high thermal conductivity, large specific surface area, and combustion-promoting characteristics of $Al_2O_3$ nanoparticles synthesized using *Syzygium cumini* leaf extract and aluminium nitrate nonahydrate ($Al(NO_3)_3 \cdot 9H_2O$). These nanoparticles improve fuel atomization, accelerate evaporation, and promote more homogeneous air-fuel mixing inside the combustion chamber. Consequently, combustion becomes more complete, increasing the amount of useful energy extracted from the fuel and reducing the quantity of fuel required to brake power output. Stable dispersion of 40 ppm $Al_2O_3$ nanoparticles further contributes to efficient combustion throughout the engine operating range.

Fig. 8 illustrates maximum BSFC of B25 blend with and without 40 ppm $Al_2O_3$ NPs at ratio of 15:1, 17:1, and 19:1. At high engine load (11 kg), the B25 + 40 ppm $Al_2O_3$ blend recorded BSFC of 0.348, 0.323, and 0.306 kg $kW^{-1}$ $h^{-1}$, whereas corresponding B25 blend exhibited 0.365, 0.342, 0.326 kg $kW^{-1}$ $h^{-1}$, respectively. Inclusion of $Al_2O_3$ NPs lowered BSFC 4.66%, 5.56%, and 6.13% at compression ratios of 15:1, 17:1, and 19:1, respectively. These results demonstrate that nanoparticle-assisted hybrid biodiesel enhances combustion efficiency and improves fuel economy under varying compression ratios.

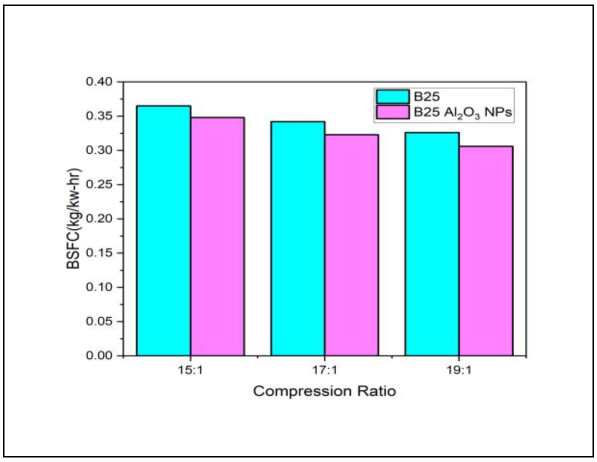


**Fig. 8: Maximum BSFC of B25 and B25 + 40 ppm $Al_2O_3$ blends**

Figure 9 presents the comparison of the highest BSFC for the B50 hybrid biodiesel blend with and

Article in Press

without 40 ppm $Al_2O_3$ nanoparticles at ratios of 15:1, 17:1, and 19:1.

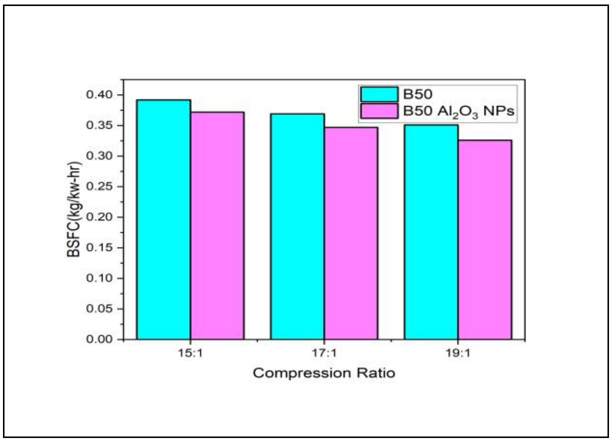


**Fig. 9: Maximum BSFC comparison of B50 and B50 + 40 ppm $Al_2O_3$ blends**

At the maximum engine load (11 kg), the B50 + 40 ppm $Al_2O_3$ blend recorded BSFC of 0.372, 0.347, and 0.326 kg $kW^{-1}$ $h^{-1}$ at compression ratios of 15:1, 17:1, and 19:1, respectively. Under the same operating conditions, the corresponding B50 blend exhibited BSFC of 0.392, 0.369, and 0.351 kg $kW^{-1}$ $h^{-1}$. Incorporation of $Al_2O_3$ NPs lowered the maximum BSFC by 5.10%, 5.96%, and 7.12%, respectively. The reduction in fuel consumption is attributed to improved fuel atomization, enhanced thermal conductivity, and more efficient combustion promoted by the $Al_2O_3$ nanoparticles synthesized using *Syzygium cumini* leaf extract and aluminium nitrate nonahydrate ($Al(NO_3)_3 \cdot 9H_2O$). These improvements enabled better utilization of the fuel energy and contributed to lower fuel consumption under all compression ratios, demonstrating the effectiveness of nanoparticle-assisted hybrid biodiesel in compression ignition engines.

## 3.2 Performance of the CatBoost Regression Models

This section evaluates the predictive capability of the developed CatBoost regression models for BTE and BSFC. The experimental dataset consisting of 108 operating conditions was divided into 20% testing and 80% training subsets. Separate CatBoost regression models were developed for BTE and BSFC prediction using biodiesel blend percentage, $Al_2O_3$ nanoparticle concentration, compression ratio, engine load, lower heating value, and brake power as predictor variables.

The predictive performance of the developed models was assessed by coefficient of determination ($R^2$), root mean square error (RMSE), mean absolute error (MAE), and mean absolute percentage error (MAPE). The obtained statistical indices demonstrate the excellent capability of CatBoost in capturing nonlinear relationships between engine operating parameters and efficiency characteristics.

**Table 6. Performance evaluation of CatBoost regression models**

| Output | $R^2$ | MAE | RMSE | MAPE (%) |
|---|---|---|---|---|
| BTE | 0.9967 | 0.2961 | 0.3884 | 1.353 |
| BSFC | 0.9918 | 0.007993 | 0.013138 | 1.730 |

Although the test-set $R^2$ values were high—0.9967 for BTE and 0.9918 for BSFC—the dataset contained only 108 observations. Therefore, these results demonstrate strong interpolation within the investigated dataset but do not independently exclude overfitting or establish performance for external datasets

The CatBoost model developed for BTE prediction achieved $R^2$ value of 0.9967, showing that approximately 99.67% of variability at experimental data were successfully explained by the model. Similarly, the BSFC model yielded an $R^2$ value of 0.9918, confirming excellent predictive capability. The low RMSE, MAE, and MAPE values further demonstrate that the prediction errors remained minimal throughout the operating range. In previous study, hybrid $Al_2O_3$–$TiO_2$ and GO–$CeO_2$ nanoparticles combined with Nannochloropsis biodiesel (B20) and CNG at a dual-fuel PCCI engine reduced brake-specific energy consumption by 8–14. CatBoost, Random Forest, and XGBoost reached high prediction ($R^2$ = 0.98–0.995) for engine performance and emission modeling (Al Awadh and Michael, 2026). These results indicate that CatBoost effectively learned the nonlinear interaction among biodiesel blend composition, nanoparticle dosage, compression ratio, and engine load.

## 3.3 Experimental Versus Predicted Performance

Figures 10(a) and 10(b) compare the experimental and CatBoost-predicted values for BTE and BSFC obtained from the testing dataset.

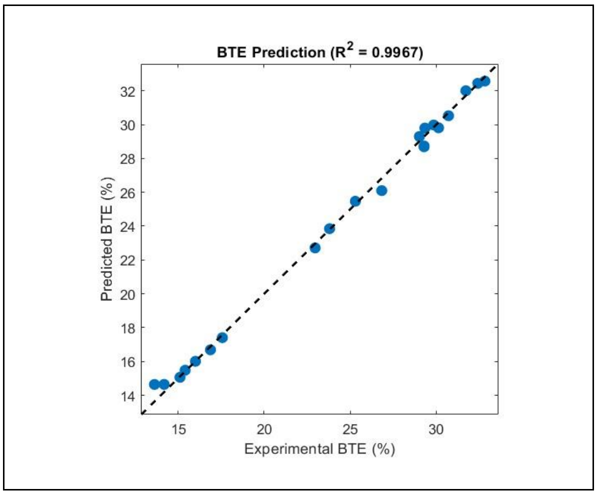


Article In Press

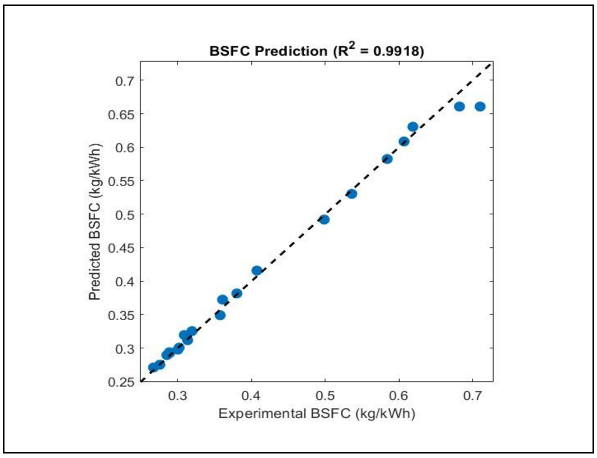


**Fig. 10: Experimental and predicted values of BTE and BSFC**

The data points are closely distributed around 45° reference line, showing excellent agreement between measured and predicted values. Only minor deviations are observed at a few operating conditions, demonstrating close agreement within the held-out test subset. However, this plot alone cannot exclude overfitting or demonstrate generalization to independent engine datasets.

The BTE prediction plot exhibits a nearly perfect linear distribution with minimal scatter, whereas the BSFC prediction plot also demonstrates excellent correlation despite the relatively smaller numerical range of BSFC values. The obtained prediction accuracy confirms that CatBoost is suitable for modeling nonlinear engine performance data generated from hybrid biodiesel fuels.

### 3.4 Residual Error Analysis

Residual analysis was performed to further verify the robustness of the developed CatBoost models. The residual error is defined as the difference between experimental and predicted values. As shown in Fig. 11(a), the BTE residuals were distributed around the zero-reference line over the predicted BTE range.

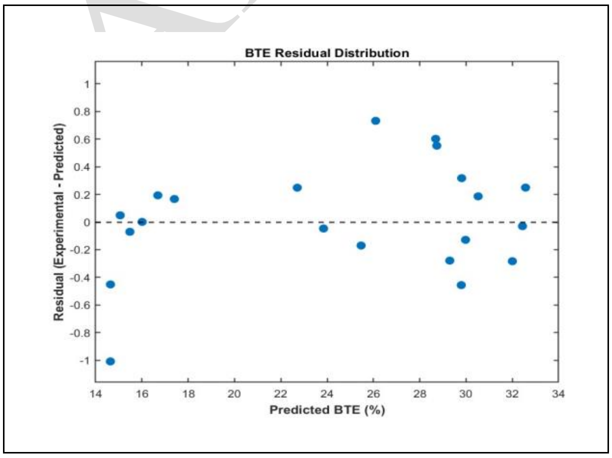


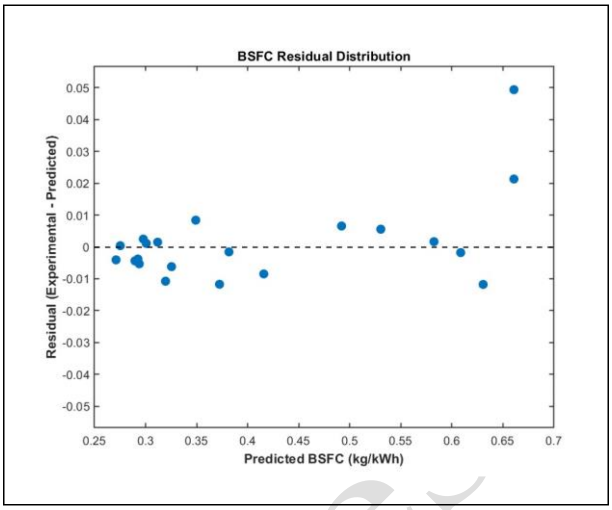


**Fig. 11: Residual plots for the predicted (a) BTE and (b) BSFC responses**

Most residuals remained between approximately −0.5 and 0.75 percentage points, although one relatively larger negative deviation of approximately −1.0 percentage point was observed at the lower BTE range. No continuous trend was evident with increasing predicted BTE, indicating that the model did not consistently overpredict or underpredict BTE. This random distribution supports the satisfactory generalization capability of the model.

Similarly, the BSFC residuals shown in Fig. 11(b) were concentrated close to zero over most of the predicted range. The larger residuals near a predicted BSFC of approximately 0.66 kg $kW^{-1}$ $h^{-1}$ corresponded to low-load operating points. In contrast, the reported BSFC values of approximately 0.306–0.392 kg $kW^{-1}$ $h^{-1}$ corresponded to the maximum load of 11 kg. Nevertheless, the errors remained small relative to the complete BSFC range and did not exhibit a clear systematic pattern. These observations agree with the low RMSE, MAE, and MAPE values obtained for the BSFC model.

The random dispersion of the residuals around zero confirms that improved models adequately captured relationships between selected engine operating variables and the corresponding performance responses. The residual analysis therefore supports the accuracy indicated by the high $R^2$ values obtained for BTE and BSFC.

### 3.5 Feature Importance Analysis

Feature-importance scores quantify the relative influence of each predictor on model predictions within the present dataset. These scores indicate predictive association and should not be interpreted as evidence of causal effects on engine performance. LHV and brake power were included as measured operating variables;

Article In Press

however, both are mathematically related to BTE and BSFC. Their inclusion may therefore increase predictive accuracy through target-related information. Accordingly, the reported models are interpreted as performance-interpolation models within the measured dataset rather than fully independent predictive models. Biodiesel blend percentage also contributes significantly owing to the variations in fuel properties with increasing biodiesel concentration. In contrast, $Al_2O_3$ nanoparticle concentration exhibits comparatively lower importance because only two dosage levels (0 and 40 ppm) were investigated. Nevertheless, nanoparticle addition still contributed positively toward improving prediction accuracy.

**Table 7. Relative importance of predictor variables obtained from CatBoost**

| Predictor | BTE (%) | BSFC (%) |
|---|---|---|
| Engine load | 31.4 | 34.2 |
| Brake power | 24.8 | 26.3 |
| Compression ratio | 18.6 | 17.5 |
| Biodiesel blend (%) | 14.3 | 12.8 |
| LHV | 7.2 | 6.5 |
| $Al_2O_3$ concentration | 3.7 | 2.7 |

Superior performance of the CatBoost models was attributed to the ability of gradient boosting decision trees to efficiently capture nonlinear interactions between engine conditions and fuel properties. Unlike conventional regression techniques, CatBoost sequentially minimizes prediction errors while incorporating regularization mechanisms that reduce overfitting. That trends with the incorporation of $Al_2O_3$ nanoparticles into B20 dairy milk scum biodiesel, CatBoost outperformed Random Forest in predicting engine efficiency and emission properties (Modi *et al.* 2025).

High prediction accuracy obtained in the present study demonstrates that CatBoost provides reliable estimates of both BTE and BSFC over the investigated operating range. Such predictive capability reduces the need for extensive experimental trials and offers a computationally efficient tool for engine performance assessment. The developed models may provide a basis for future optimization studies; however, no optimization algorithm or independently validated optimum operating condition was established in the present investigation.

### 3.6 Emission Analysis and Environmental Impact

The present study mainly evaluated the engine efficiency of hybrid biodiesel through BTE and BSFC. Nevertheless, environmental implications of incorporating $Al_2O_3$ nanoparticles into hybrid biodiesel prepared from rubber seed oil and avocado seed oil were also important for assessing its suitability as a sustainable alternative fuel. Although exhaust emissions were not experimentally measured in this investigation, previous research has shown that $Al_2O_3$ NPs improve combustion efficiency by promoting finer fuel atomization, enhanced air-fuel mixing, and more complete oxidation of fuel (Gopidesi *et al.* 2025).

The $Al_2O_3$ nanoparticles synthesized using *Syzygium cumini* leaf extract and aluminium nitrate nonahydrate ($Al(NO_3)_3 \cdot 9H_2O$) are expected to enhance combustion stability without adversely affecting fuel properties. The influence on nitrogen oxides ($NO_x$) may vary because higher combustion temperatures can increase thermal $NO_x$ formation, whereas shorter combustion duration and improved oxidation may partially offset this effect. Therefore, future investigations will include a comprehensive analysis of exhaust emissions to validate environmental benefits of $Al_2O_3$ nanoparticle-improved hybrid biodiesel under various engine operating conditions.

## 4. CONCLUSIONS

A rubber seed–avocado seed hybrid biodiesel was prepared in an equal 1:1 proportion and enhanced with 40 ppm $Al_2O_3$ nanoparticles synthesized using *Syzygium cumini* leaf extract. Nanoparticle formation was preliminarily supported by the UV–visible absorption near 350 nm, the Al–O FTIR vibration near 595 $cm^{-1}$, and a DLS particle size of 30 ± 5 nm. The novelty of the study lies in integrating this hybrid biodiesel–nanoparticle system with CatBoost-based performance prediction. At the maximum load of 11 kg, B25 + $Al_2O_3$ increased BTE by 6.10% and reduced BSFC by 6.13% at a compression ratio of 19:1. B50 + $Al_2O_3$ produced a maximum BTE improvement of 6.05% at 17:1 and a maximum BSFC reduction of 7.12% at 19:1. The CatBoost models achieved $R^2$ values of 0.9967 for BTE and 0.9918 for BSFC using 108 operating conditions and an 80:20 train–test split. These results demonstrate improved BTE and BSFC for B25 and B50 within the investigated conditions of 1500 rpm, loads of 2–11 kg, compression ratios of 15:1–19:1, and an $Al_2O_3$ concentration of 40 ppm. However, the nanoparticle crystalline phase, direct combustion behaviour, exhaust emissions, and external model generalizability were not established. Future work should include XRD and SEM/TEM–EDX characterization, combustion and emission measurements, validation using larger datasets, and independent optimization of the fuel and engine parameters. In addition, the integration of CatBoost provides an efficient predictive framework that can minimize experimental effort and support future optimization of nanoparticle-assisted biodiesel formulations for sustainable engine applications.

## FUNDING

Article In Press

This research received no specific grant from any funding agency in the public, commercial, or not-for-profit sectors.

## CONFLICTS OF INTEREST

The authors declare that there is no conflict of interest.

## COPYRIGHT

This article is an open-access article distributed under the terms and conditions of the Creative Commons Attribution (CC BY) license (http://creativecommons.org/licenses/by/4.0/).

## REFERENCES

Al Awadh, M. and Michael, G. K. O., RSM optimisation and explainable machine learning of a CNG–diesel–Nannochloropsis B10/B20 Fueled PCCI engine with hybrid nanoparticles, *Appl. Therm. Eng.*, 298, 131019 (2026). https://doi.org/10.1016/j.applthermaleng.2026.131019

Al Zubi, M. A., Penmetsa, R. V, Kumar, P. S., Patil, P. P., Singh, B., Alsubih, M., Islam, S. and Khan, W. A., Performance and emission characteristics of novel biodiesel-diesel blends: An RSM and ANN approach, *Int. J. Low-Carbon Technol.*, 19, 1060–1077 (2024). https://doi.org/10.1093/ijlct/ctae025

Amale, A. B., Satishkumar, P., Bhagat, P. R., Motghare, M. S. and Krishnaraj, C., Green Synthesis of ZnO Nanoparticles Using Azadirachta indica Leaf Extract for Rapid Catalytic Degradation of Organic Pollutants, *J. Environ. Nanotechnol.*, 15(2), 151–161 (2026). https://doi.org/10.13074/jent.2026.06.2612082

Bilal, F. S., Elumalai, P. V, Mishra, N. K., Chan, C. K., Saleel, C. A., Hussain, F., Khan, S. A. and Keçebaş, A., Hydrogen-enriched dual-fuel CI engine fueled with Mahua biodiesel and hybrid nano-additives: Integrated experiments, explainable machine learning, and multi-objective optimization, *Int. J. Hydrogen Energy*, 235, 155037(2026). https://doi.org/10.1016/j.ijhydene.2026.155037

Borsato, D., Mantovani, A. C. G., Chendynski, L. T., Angilelli, K. B. and Romagnoli, É. S. Thermal Degradation Monitoring of Biodiesel in the Presence and Absence of Alcoholic Extract of Jambolan (*Syzygium cumini* Lamarck) and $Cu^{2+}$ Ions by 1H NMR Spectroscopy, *Quimica Nova*, 49(2026). https://doi.org/10.21577/0100-4042.20260052

Bukkarapu, K. R. and Krishnasamy, A., Machine learning-driven biodiesel feedstock selection for improved engine performance and emission control, *Int. J. Engine Res.*, 9801(2026). https://doi.org/10.1177/14680874261429801

Dhairiyasamy, R., Dixit, S., Singh, S. and Gabiriel, D., A comprehensive analysis of combustion efficiency and emissions in biodiesel blends for sustainable energy solutions, *Int. J. Thermoflu.*, 29, 101357(2025). https://doi.org/10.1016/j.ijft.2025.101357

Dheenathayalan, T., Kandasamy, M. and Vellaiyan, S., Valorization of Carica papaya seed oil into biodiesel using a stable CuO–$Al_2O_3$ nanocatalyst under optimized condition, *Sustain. Chem. Pharm.*, 48, 102207 (2025). https://doi.org/10.1016/j.scp.2025.102207

Dinesh, K. V., Hemadri, B. V., Sugumaran, C., Vinodhkumar, B. and Kumar, S. S., Synergistic Effect of $Al_2O_3$ Nanoparticles on the Performance and Emission Characteristics of an Optimum B25 Biodiesel Blend in a Diesel Engine, *J. Environ. Nanotechnol.*, 14(4), 143–152 (2025). https://doi.org/10.13074/jent.2025.12.2541879

Gopidesi, R. K., Uttamrao, K. N., Naik N., C. K., S R, P., Hadi, A. A., Sunil Kumar, K., Khan, T. M. Y., Shaik, A. S. and Alamiery, A. A., Optimization of compression ratio in LHR engine fueled with nano $Al_2O_3$-emulsified biodiesel using RSM and machine learning, *RSC Adv.*, 15(59), 51178–51197(2025). https://doi.org/10.1039/d5ra06361b

Kannappan, C., Sengottaiyan, S. and Ramasamy, R., Effects of hydrogen enrichment on the performance and emission characteristics of a diesel engine with the addition of *Syzygium cumini* (Jamun) biodiesel, *Austra. J. Mech. Eng.*, 23(4), 774–780 (2025). https://doi.org/10.1080/14484846.2024.2408071

Kannappan, C., Sengottaiyan, S. and Ramasamy, R., The combined effect of EGR and hydrogen addition on a *Syzygium cumini* (jamun) liquid biofuel engine, *Biotechnol. Biofuels Bioprod.*, 16(1), 105(2023). https://doi.org/10.1186/s13068-023-02330-2

Li, J., Dong, Q. and Wang, H., Hybrid machine learning-based modeling of engine behavior using third-generation biodiesel: validation and robustness with SHAP explainability, bootstrapping, and sensitivity analysis, *Appl. Therm. Eng.*, 281, 128502(2025). https://doi.org/10.1016/j.applthermaleng.2025.128502

Modi, V., Rampure, P. B., Shetty, S. K., Nagaral, M., Naik N, C. K., M. G. M, J., Abdullah, M. I., Al-Mansour, A. I. and Alam, S., Nano-Enhanced Dairy Scum Biodiesel Blends: Unleashing the Power of Aluminium Oxide for Sustainable and Efficient Engine Performance, *J. Therm. Sci.*, 34(1), 283–302 (2025). https://doi.org/10.1007/s11630-024-2055-4

Munir, M., Ahmad, M., Abdullah Alsahli, A., Zhang, L., Islamov, S., Sultana, S., Ussemane Mussagy, C., Mustafa, A., Munir, M., Chaudhry, B., Hamayun, M.

Article In Press

and Khawaja, S., Harnessing non-edible Quercus incana seeds for sustainable and clean biodiesel production using seed-derived green $Al_2O_3$ nanocatalyst, *Sustain. Energy Technol. Assess.*, 72, 104025 (2024). https://doi.org/10.1016/j.seta.2024.104025

Oni, B. A., Sanni, S. E., Ibegbu, A. J. and Oguntade, T. I., Authentication of Styrax officinalis L. methyl ester nanoparticulate fuel-system's suitability in powering CI engines, *Indus. Crops Prod.*, 181, 114833 (2022). https://doi.org/10.1016/j.indcrop.2022.114833

Rajakannu, A., Sengodan, N., Tonk, A., Vimal, A., Subbulakshmi, R., Giri, R. and Mayakannan, S., Evaluation of Machine Learning Models in Predicting Diesel Engine Behaviour and Emissions with Biodiesel Blends, *Int. J. Veh. Struct. Syst.*, 17(3), 449–455 (2025). https://doi.org/10.4273/ijvss.17.3.12

Renish, R. R. and Amala, J. S. M., An Investigation into the Impact of Nano-Additives on the Performance and Emission Levels of a Diesel Engine Fuelled by Nahar Biodiesel, *J. Environ. Nanotechnol.*, 13(3), 408–417 (2024). https://doi.org/10.13074/jent.2024.09.243823

Sai, B. A. V. S. L., Niju, S., Meera, S. B. K. M. and Anantharaman, N., Process parameter optimisation in acid value minimisation of rubber seed oil conversion to biodiesel using $Al_2O_3$/Calcined Eggshells as catalyst–RSM and ANN studies, *Int. J. Amb. Energy*, 43(1), 3200–3207 (2022). https://doi.org/10.1080/01430750.2020.1818125

Saravanakumar, V., Balu, P., Saravanan, C. and Krishnan, P. N., The Influence of Various Nano-Additives on Performance, Emission and Combustion Characteristics of *Syzygium cumini* (Jamun) Biodiesel Fuelled DI Engine, *Renewable Energy Res. Appli.*, 6(2), 213–220 (2025). https://doi.org/10.22044/rera.2025.14460.1315

Sasikumar, B., Jeevanandam, P., Samikkannu, V. B. and Veeramalini, J. B., Transesterification Studies on Avocado Seed Oil Using Carbon Supported CuO Nano Catalyst: Rate Kinetics and Thermodynamic Aspects, *J. Nanomater.*, 2022(1), 5192239(2022). https://doi.org/10.1155/2022/5192239

Sengodan, N., Mayakannan, S., Venugopal, K. and Raja, T., Performance and Analysis of RCCI Combustion using Gasoline and Jatropha Curcas Biodiesel for Enhanced Efficiency and Reduced Emissions in CI Engines, *Int. J. Veh. Struct. Syst.*, 17(3), 506–519 (2025). https://doi.org/10.4273/ijvss.17.3.20

Siam, M. T. R., Siddiki, M. N. A. and Islam, M. A., Engine performance and emission analysis of optimized biodiesel produced from tobacco seed oil utilizing $Al_2O_3$-CuO hybrid nano additives, *Energy Convers. Manage. X*, 30, 101544(2026). https://doi.org/10.1016/j.ecmx.2026.101544

Suprihatin, Rahmandika, A. J. P. and Fikri, M., Synthesis of Avocado Seeds into Biodiesel Using a Catalyst CaO from Blood Cockle Shell, *Adv. Sustain. Sci. Eng. Technol.*, 6(4), 0240404(2024). https://doi.org/10.26877/asset.v6i4.779

Tesfaye, L. M., Seyoum, Z. D. and Yitayew, K. B., A comparative study on the effect of nano-additives on performance and emission characteristics of CI engine run on castor biodiesel blended fuel, *Energy Convers. Manage. X*, 20, 100493(2023). https://doi.org/10.1016/j.ecmx.2023.100493

Thangam, R. K., Velmurugun Parameswari, S., Moranahalli Ponnusamy, S. K. and Jayavel, M., Production of rubber seed oil biodiesel using biomass derived catalyst and engine performance, combustion and emission characteristics with hydrogen dual fuel and alumina additive, *Appl. Therm. Eng.*, 286, 129402(2026). https://doi.org/10.1016/j.applthermaleng.2025.129402

Yatish, K. V., Prakash, R. M., Ningaraju, C., Sakar, M., GeethaBalakrishna, R. and Lalithamba, H. S., Terminalia chebula as a novel green source for the synthesis of copper oxide nanoparticles and as feedstock for biodiesel production and its application on diesel engine, *Energy*, 215, 119165(2021). https://doi.org/10.1016/j.energy.2020.119165

Article in Press